Manganese(I) complexes with metal-to-ligand charge transfer luminescence and photoreactivity

Patrick Herr, Christoph Kerzig, Christopher B. Larsen, Daniel Häussinger and Oliver S. Wenger*

Department of Chemistry, University of Basel, St. Johanns-Ring 19, 4056 Basel, Switzerland

Abstract

Precious metal complexes with the d^6 valence electron configuration often exhibit luminescent metal-to-ligand charge transfer (MLCT) excited states, which form the basis for many applications in lighting, sensing, solar cells, and synthetic photochemistry. Iron(II) has received much attention as a possible Earth-abundant alternative, but to date no iron(II) complex has been reported to show MLCT emission upon continuous-wave excitation. Manganese(I) has the same electron configuration as iron(II), but had typically been overlooked in the search for cheap MLCT luminophores until now. Here we report that isocyanide chelate ligands give access to air-stable manganese(I) complexes that exhibit MLCT luminescence in solution at room temperature. These compounds were successfully used as photosensitizers for energy- and electron-transfer reactions and were shown to promote the photoisomerization of trans-stilbene. The observable electron transfer photoreactivity occurred from the emissive MLCT state, whilst the triplet energy transfer photoreactivity originates from a ligand-centered $^3\pi$-π^* state.

Introduction

The long-lived MLCT excited states of many Ru(II) and Ir(III) complexes play key roles in light-emitting devices[1], dye-sensitized solar cells[2], photoredox catalysis[3], artificial photosynthesis[4] and photodynamic therapy[5]. There is a long-standing interest in replacing these precious and rare $4d^6$ and $5d^6$ ions by cheaper $3d^6$ elements, and until now essentially all efforts in that direction concentrated on Fe(II)[6]. However, the MLCT states of Fe(II) complexes deactivate on very rapid timescales, due to metal-centered (MC) excited states situated at much lower energies than in Ru(II) or Ir(III)[7-11]. Recently, these undesired deactivation processes were decelerated by innovative molecular design[12,13], yet no MLCT luminescence after continuous-wave excitation has been reported to date[14,15]. In the course of these efforts, ligand-to-metal charge transfer (LMCT) luminescence from Fe(III) ($3d^5$) complexes was discovered[16,17],

but the direction of charge transfer is important for many applications hence emissive MLCT states of $3d^6$ complexes remain a strategic key target[18]. In particular, the development of $3d^6$ complexes resembling the prototypical $[Ru(bpy)_3]^{2+}$ compound (bpy = 2,2'-bipyridine) both structurally and functionally represents a grand challenge[19]. We recently reported a very weakly luminescent Cr(0) complex, but that compound suffered from sensitivity to air due to facile oxidation of Cr(0)[20]. For the present study, we turned to isoelectronic Mn(I), for which some air-stable complexes with π-acceptor ligands had been known[21-23]. After iron and titanium, manganese is the third most abundant transition metal element, exceeding the natural abundance of copper by a factor of 18, which seems noteworthy because copper has received much attention from the photophysics and photochemistry community[24-27]. The abundance and low cost combined with the prospect of obtaining compounds with low toxicity recently triggered interest in Mn(I) complexes as catalysts for C-H activation[28] and other applications in organic chemistry[29,30], as well as for electrocatalytic CO_2 reduction related to artificial photosynthesis[31,32]. Well-known tricarbonyl complexes of Mn(I) are non-luminescent,[33] and the photophysics of homoleptic Mn(I) complexes is as yet essentially unexplored. Our Mn(I) photosensitizers complement recent important discoveries of LMCT luminophores made from Earth-abundant metals (including a Mn(IV) complex)[16,17,34-36], and they represent the first air-stable $3d^6$ complexes with luminescent MLCT states. The Mn(I) complexes presented herein furthermore have a low-lying ligand-centered $^3\pi$-π^* state, which leads to unexpectedly rich photophysics and photochemistry of this new class of compounds.

Results and discussion

Molecular design, synthesis and characterization

Isocyanide ligands can stabilize metals in low oxidation states[37], and monodentate arylisocyanides provided access to emissive W(0) complexes in earlier studies[38,39]. Since chelate ligands usually give more robust coordination compounds, we previously developed bidentate isocyanide ligands with terphenyl backbones to obtain photoactive Cr(0) and Mo(0) complexes[20,40]. For the Mn(I) complexes reported herein (Fig. 1), we synthesized two isocyanide chelates (Supplementary Information) with thiophene units in the backbone to optimize bite angles, one of them bidentate (L^{bi}) and the other tridentate (L^{tri}). The free ligands reacted with $Mn(CO)_5Br$ to the homoleptic complexes $[Mn(L^{bi})_3]^+$ and $[Mn(L^{tri})_2]^+$ (Fig. 1), which were characterized with all standard techniques (Supplementary Information) including ^{55}Mn NMR spectroscopy. The ^{55}Mn NMR shifts of $[Mn(L^{bi})_3]^+$ and $[Mn(L^{tri})_2]^+$ were

determined as δ = –1225 and –1419 ppm, respectively, and fall both unambiguously in the range –1000 > δ > –1500 for Mn(I) complexes[41]. L^{tri} binds in meridional fashion, and the direct comparison of bis(tridentate) and tris(bidentate) coordination environments allowed us to probe differences in robustness and photophysical behavior.

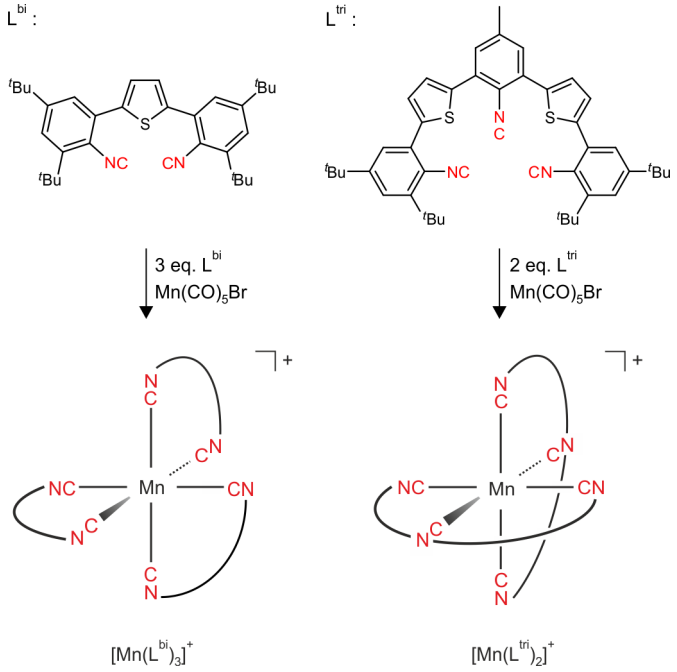

Figure 1. Molecular structures of the ligands and complexes (isolated as PF_6^- salts) explored in this work. Yields for complexation: 64% for $[Mn(L^{bi})_3]^+$, 41% for $[Mn(L^{tri})_2]^+$.

Photoluminescence and electronic structure

Both complexes are yellow due to an absorption band near 400 nm (solid purple lines in Fig. 2 / Supplementary Fig. 24), which tails to the deep blue region and is not present in the free ligands (dotted purple lines). Excitation into this absorption band causes solvatochromic luminescence, which red-shifts by roughly 1500 cm^{-1} between toluene and CH_3CN. In some solvents Raman-scattered excitation light is detectable (asterisks in Fig. 2 / Supplementary Fig. 24), but the emission bands are unstructured. The luminescence quantum yields (ϕ) in deaerated CH_3CN at 20 °C are 0.05% for $[Mn(L^{bi})_3]^+$ and 0.03% for $[Mn(L^{tri})_2]^+$ (Supplementary Information), which is more than one order of magnitude higher than for our recently reported Cr(0) complex emitting from a ^{3}MLCT state[20], whereas Fe(II) complexes are completely non-emissive under comparable conditions. The presence of low-lying metal-centered (MC) excited states in the $3d^6$ configuration makes it much harder to establish luminescent charge-transfer excited states than in the $3d^0$ and $3d^{10}$ configurations, in which MC states are absent. Thus, the step from no luminescence (as in all

previously studied Fe(II) complexes) to weak MLCT emission in our Mn(I) complexes represents an important breakthrough.

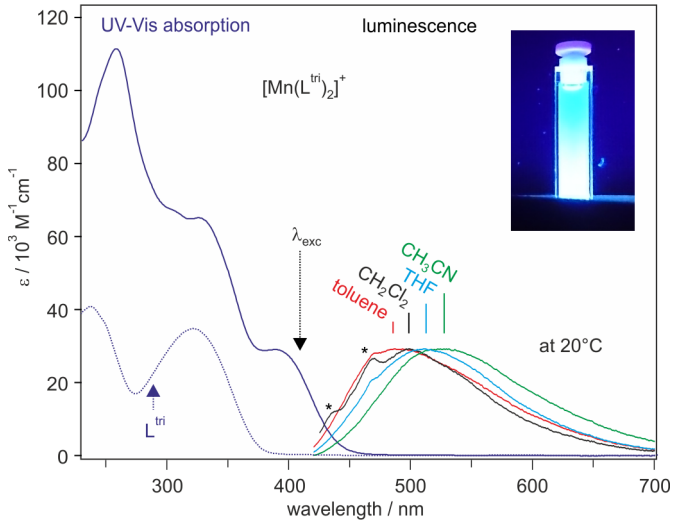

Figure 2. Steady-state absorption and emission spectroscopy. Left, purple lines: UV-Vis absorption spectra of $[Mn(L^{tri})_2]^+$ (solid) and L^{tri} (dotted) in CH_2Cl_2. Right: Luminescence spectra of $[Mn(L^{tri})_2]^+$ following excitation at 410 nm (λ_{exc}) in four different de-aerated solvents. The asterisks mark peaks caused by Raman scattered excitation light. Top right: Cuvette with a solution of $[Mn(L^{tri})_2]^+$ in CH_3CN irradiated from the bottom by a UV lamp for chromatography (λ_{exc} = 366 nm).

In picosecond transient absorption spectroscopy a ground-state bleach is observable near 400 nm (Fig. 3a / Supplementary Fig. 25) and an excited-state absorption band appears at 470 nm. Following pulsed excitation, the excited-state absorption at 470 nm and the luminescence at 460 nm show very similar decay behavior (Fig. 3d / Supplementary Fig. 25), indicating that both signals belong to the same excited state. MLCT states are formally comprised of an oxidized metal and a reduced ligand, whose individual spectral signatures are accessible via spectro-electrochemistry[42]. In our complexes, Mn(I) is oxidized reversibly to Mn(II) at ca. 1.0 V vs SCE (Fig. 3f / Supplementary Fig. 25), in line with expectation (Supplementary Information)[21-23]. Reductive sweeps (Fig. 3e / Supplementary Fig. 25) contain several irreversible waves, the first one of which (at -1.9 V vs SCE) is attributable to the reduction of coordinated L^{tri}/L^{bi} to $(L^{tri})^{\bullet-}/(L^{bi})^{\bullet-}$. At a constant potential of -2.2 V vs SCE, the spectro-electrochemical $(L^{tri})^{\bullet-} - L^{tri}$ (Fig. 3b) and $(L^{bi})^{\bullet-} - L^{bi}$ (Supplementary Fig. 25) difference spectra are obtained. At a fixed potential of 1.2 V vs SCE, one obtains the spectro-electrochemical difference spectra in Fig. 3c / Supplementary Fig. 25, which correspond to the subtraction of spectra of Mn(I) from Mn(II) species. The picosecond transient

absorption spectra (Fig. 3a) are essentially a linear combination of the difference spectra of metal oxidation (Fig. 3c) and ligand reduction (Fig. 3b), as expected for MLCT transitions[42]. This very good agreement between transient absorption and spectro-electrochemical data (for metal-based oxidation and ligand-centered reduction) is compatible with an electronically excited state that has strong MLCT character.

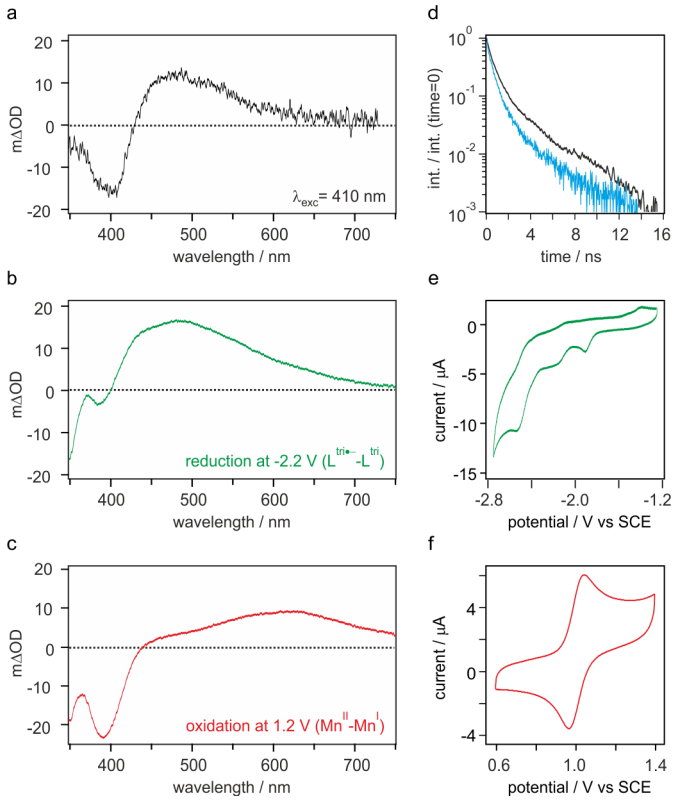

Figure 3. Time-resolved and (spectro-)electrochemical data for $[Mn(L^{tri})_2]^+$. **a**, UV-Vis transient difference spectrum of 16 µM $[Mn(L^{tri})_2]^+$ in de-aerated CH_2Cl_2 at 20 °C, time-integrated over 2 ns following excitation at 410 nm with 30-ps laser pulses. **b**, UV-Vis changes upon electrochemical (ligand-centered) reduction in CH_3CN. **c**, UV-Vis changes upon electrochemical (metal-centered) oxidation in CH_3CN. **d**, Decays of the excited-state absorption signal at 470 nm (black, λ_{exc} = 410 nm) and the luminescence intensity at 460 nm (blue, λ_{exc} = 405 nm) in de-aerated CH_2Cl_2 at 20 °C. **e**, Cyclic voltammogram showing ligand-based reduction in deaerated CH_3CN. **f**, Cyclic voltammogram showing metal-based oxidation in CH_2Cl_2. The electrolyte was 0.1 M $TBAPF_6$, all potentials are given against the saturated calomel electrode (SCE).

Luminescence lifetimes are tri-exponential with weighted average lifetimes of 0.74 ns for $[Mn(L^{bi})_3]^+$ and 1.73 ns for $[Mn(L^{tri})_2]^+$ in deaerated CH_3CN at 20 °C (Table 1), close to some of the longest lifetimes for (dark) MLCT states in Fe(II) complexes[12,13], and similar to the MLCT lifetime (2.2 ns) of our recently reported Cr(0) isocyanide complex[20].

The backbones of our ligands L^{tri} and L^{bi} contain sequences of CNAr-thiophene-ArNC units, and flipping of the central thiophene unit with respect to the neighboring ArNC (arylisocyanide) units can lead to different conformers (Supplementary Information), and this causes the multi-exponential decay behavior[40]. All three decay components (τ_1, τ_2, τ_3) have identical luminescence spectra (Supplementary Figs. 32/33), which is in line with a single emissive state in different conformers.

Table 1. Electrochemical and photophysical parameters[a].

	$[Mn(L^{bi})_3]^+$	$[Mn(L^{tri})_2]^+$
E^0 ($Mn^{II/I}$) vs SCE [b]	1.05 V	1.00 V
E^0 (($L^{tri/bi}$)/($L^{tri/bi}$)$^{\bullet-}$) vs SCE	-1.94 V	-1.91 V
τ_{avg} / ns	0.74	1.73
τ_1, τ_2, τ_3 / ns [c]	0.374 (79.2%), 1.84 (19.3%), 5.85 (1.5%)	0.635 (56.4%), 2.07 (33.6%), 6.74 (10.0%)
ϕ	0.05%	0.03%

[a] In de-aerated CH_3CN at 20 °C unless otherwise noted. [b] In CH_2Cl_2 at 20 °C. $L^{tri/bi}$ denotes coordinated ligands.

[c] Values in parentheses indicate relative importance.

In isoelectronic $[Fe(bpy)_3]^{2+}$, excitation into the ^{1}MLCT absorption band is followed by intersystem crossing to the lowest ^{3}MLCT excited state within less than 20 fs[43], and from this perspective it seems plausible that the emissive MLCT states of our Mn(I) complexes (at 2.9 eV) are triplets. However, upon addition of excess naphthalene (with a triplet energy (E_T) of 2.64 eV) or *p*-terphenyl (E_T = 2.52 eV) the characteristic triplet excited-state absorption signatures of these polyaromatic hydrocarbons are not observable, even though rate constants for triplet-triplet energy transfer typically reach the diffusion-limit when the driving-force is 0.2 eV or greater[44]. Only when polyaromatic hydrocarbons with lower triplet energies such as pyrene (E_T = 2.10 eV, Supplementary Information) or anthracene (E_T = 1.85 eV, see further below) are used, there is clear evidence for triplet-triplet energy transfer. Thus, it looks as if our Mn(I) complexes have a (dark) triplet excited state below 2.52 eV (*p*-terphenyl) but above 2.10 eV (pyrene). However, upon direct excitation of the Mn(I) complexes in solution at 20°C, we were unable to detect long-lived excited states other than the MLCT in Fig. 3a / Supplementary Fig. 25.

To get direct insight into the electronic structures of our coordinated ligands (and possible low-lying ligand-centered triplet states), we explored the $[ZnCl_2(L^{bi})]$ complex (Supplementary Fig. 44). Expectedly, the UV-Vis spectrum of $[ZnCl_2(L^{bi})]$ closely resembles that of uncoordinated L^{bi}, as the MLCT absorption bands observable for the Mn(I) complexes at 400 nm (Fig. 2 / Supplementary Fig. 24) are absent for Zn(II). In solution at 20 °C, $[ZnCl_2(L^{bi})]$ exhibits luminescence with a band maximum at 440 nm (Supplementary Fig. 44), blue-shifted more than 50 nm relative to the MLCT emissions in Figs. 2 / Supplementary Fig. 24. This luminescence with a lifetime of 1.24 ns (Supplementary Fig. 45) is attributed to fluorescence from a $^1\pi$-π^* state at 3.2 eV (Fig. 4e). In our search for a low-lying $^3\pi$-π^* state, we explored one Ru(II) and three Ir(III) complexes with well-defined triplet energies as sensitizers for triplet-triplet energy transfer to $[ZnCl_2(L^{bi})]$ (Supplementary Information), in particular [Ru(1,10-phenanthroline)$_3$]$^{2+}$ ([Ru]), [Ir(2-phenylpyridine)$_2$(4,4'-di-*tert*-butyl-2,2'-bipyridine)]$^+$ ([Ir-1]), *fac*-[Ir(2-phenylpyridine)$_3$] ([Ir-2]), and *fac*-[Ir(2-(2,4-difluorophenyl)pyridine)$_3$] ([Ir-3]). Selective excitation of the Ir(III) complexes with E_T values between 2.4 and 2.7 eV in presence of excess Zn(II) complex yields a long-lived ($\tau_T > 50$ μs) photoproduct that can be assigned to triplet-excited $[ZnCl_2(L^{bi})]$ (Supplementary Fig. 47), whilst the Ru(II) complex with $E_T = 2.2$ eV fails to provide this photoproduct. From this we conclude that coordinated L^{bi} has $^3\pi$-π^* state at ca. 2.3 eV (Fig. 4e), and given the structural similarity between L^{bi} and L^{tri}, it seems reasonable to assume that this is also the case for the tridentate ligand (for which we have been unable to isolate a stable Zn(II) complex). It follows that there must be a ligand-centered $^3\pi$-π^* state at ca. 2.3 eV in $[Mn(L^{bi})_3]^+$ and $[Mn(L^{tri})_2]^+$ (Fig. 4d).

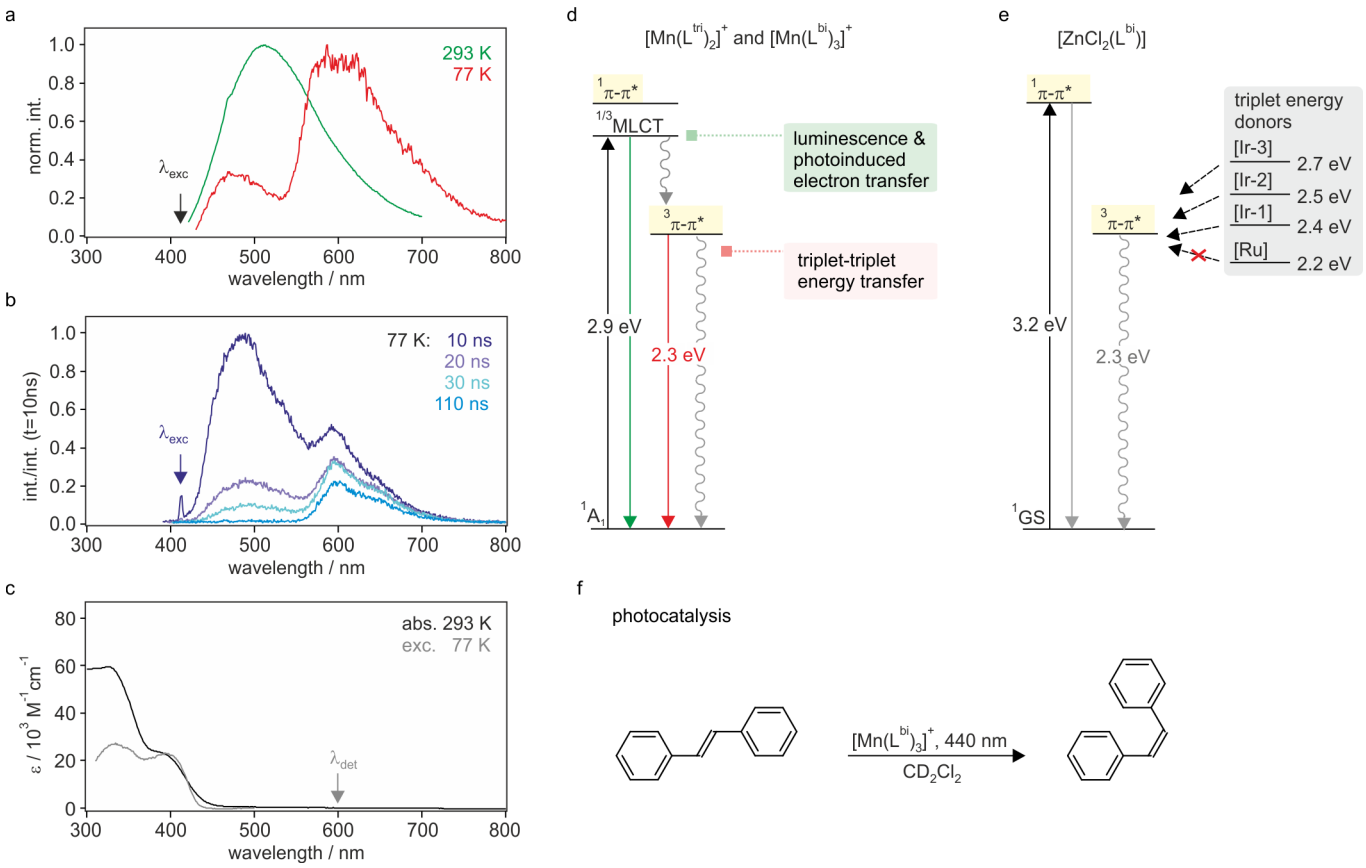

Figure 4. Dual emission at 77 K, different excited states and their photo-reactivities. **a**, Luminescence of $[Mn(L^{tri})_2]^+$ (25 µM) after continuous wave-excitation at 410 nm in de-aerated THF (293 K) and 2-methyl-THF (77 K). **b**, Luminescence at 77 K after pulsed excitation of $[Mn(L^{tri})_2]^+$ (25 µM) at 410 nm and different detection delay times but constant integration times of 1 µs. **c**, Black: UV-Vis spectrum of $[Mn(L^{tri})_2]^+$ in THF at 293 K. Gray: Excitation spectrum monitoring the 600-nm emission of $[Mn(L^{tri})_2]^+$ in 2-methyl-THF at 77 K. **d**, Energy-level scheme for the Mn(I) complexes; colored arrows represent emissions observed at 20 °C (green) and 77 K (red), respectively. Wavy arrows denote nonradiative relaxation processes. **e**, Energy-level scheme for the $[ZnCl_2(L^{bi})]$ reference complex. Determination of the $^3\pi$-π^* energy occurred with one ruthenium- ([Ru]) and three iridium-based triplet sensitizers ([Ir-1], [Ir-2], [Ir-3]) with well-defined triplet energies between 2.2 and 2.7 eV. Three of these sensitizers show triplet-triplet energy transfer to the $[ZnCl_2(L^{bi})]$ complex (black dashed arrows), one does not (black dashed arrow crossed out in red). **f**, Photoisomerization of *trans*-stilbene (50 mM) to *cis*-stilbene upon irradiation of $[Mn(L^{bi})_3]^+$ (2 mM) at 440 nm.

When exciting the Mn(I) complexes in frozen 2-methyl-THF at 77 K, one observes dual emission (red trace in Fig. 4a / Supplementary Fig. 26), with two bands with maxima at 475 and 605 nm. The higher energy band resembles the room temperature emission (green trace), but the additional low-energy band is more prominent at 77 K. In time-gated

experiments at 77 K (Figs. 4b / Supplementary Fig. 26), the intensity ratio between the two bands depends strongly on the time delay used for detection, because they have very disparate decay behavior. Whilst the 475-nm emission decays within the instrumental limit (10 ns), the 605-nm luminescence has a lifetime of 118 µs for $[Mn(L^{bi})_3]^+$ and 213 µs for $[Mn(L^{tri})_2]^+$ at 77 K (Supplementary Fig. 34). This low-energy emission clearly originates from the Mn(I) complexes, as the excitation spectra in Figs. 4c / Supplementary Fig. 26 confirm. All of these data are in line with an MLCT state at 2.9 eV, which is responsible for the room temperature emission, and a ligand-centered $^3\pi$-π^* state at ca. 2.3 eV, which only emits at low temperatures (Fig. 4d). At 20 °C, the $^3\pi$-π^* state in the Mn(I) complexes deactivates rapidly and escapes direct detection by transient absorption spectroscopy, as noted above. Possibly, ^{3}MC states deactivate the $^3\pi$-π^* state at 20 °C.

Photoinduced energy- and electron-transfer

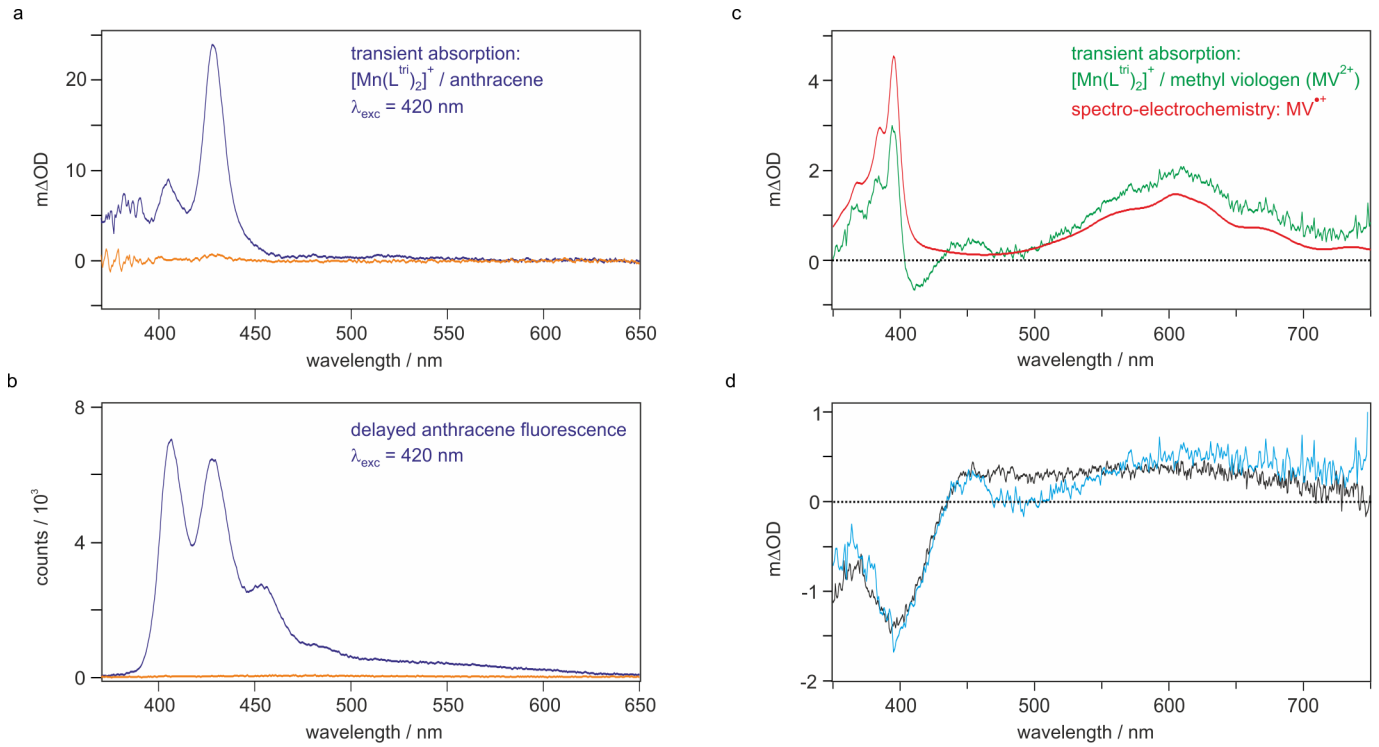

Figure 5. Photoinduced energy and electron transfer. **a**, Purple: Transient absorption spectrum after excitation of $[Mn(L^{tri})_2]^+$ (25 µM) at 420 nm in presence of 40 mM anthracene in de-aerated toluene. Orange: spectrum obtained under identical conditions without $[Mn(L^{tri})_2]^+$. **b**, Luminescence of the two solutions used in **a**. **c**, Green: Transient absorption spectrum after 420-nm excitation of $[Mn(L^{tri})_2]^+$ (25 µM) in presence of 80 mM methyl viologen (MV^{2+}) in de-aerated CH_3CN. Red: UV-Vis difference spectrum upon electrochemical reduction of MV^{2+} to $MV^{\bullet+}$. **d**, Blue:

Difference between the red and the green spectra in **c**; scaling factor chosen such that the difference between the transient absorption spectrum of $MV^{\bullet+}$ and the spectrum of the oxidized complex was as small as possible. Black: Transient absorption difference spectrum resulting from oxidation of $[Mn(L^{tri})_2]^+$ to $[Mn(L^{tri})_2]^{2+}$, obtained after 410-nm excitation of $[Mn(L^{tri})_2]^+$ (20 μM) in presence of 1 M CCl_4 in de-aerated CH_3CN. All spectra measured at 20 °C, using pulse durations and energies of 10 ns and 6 mJ, respectively. Delay and integration times were 200 ns / 200 ns for **a**, 200 ns / 500 μs for **b**, 10 ns / 200 ns for **c** and **d**.

With their luminescent MLCT states at 2.9 eV and ligand-centered $^3\pi$-π^* states at 2.3 eV, the new family of Mn(I) complexes resembles special cases of Ru(II) polypyridine compounds, in which there are non-equilibrated MLCT and $^3\pi$-π^* excited states (see Supplementary Information for a broader discussion)[45,46]. Given this electronic structure, it seemed interesting to explore their photo-reactivities. After 420-nm excitation of the Mn(I) complexes in presence of 80 mM methyl viologen (MV^{2+}) in CH_3CN, they undergo electron transfer to form Mn(II) and $MV^{\bullet+}$ (Figs. 5c / Supplementary Fig. 27). Subtraction of the $MV^{\bullet+}$ contribution (red traces) from the transient absorption spectra (green traces) yields the blue traces in Figs. 5d / Supplementary Fig. 27. The latter are in agreement with transient difference spectra from a separate experiment, in which the Mn(I) complexes were photo-oxidized to Mn(II) in presence of CCl_4 (black traces)[47]. Based on Mn(I/II) potentials of ca. 1.0 V vs SCE (Table 1) and an energy of ca. 2.9 eV for the luminescent state (Figs. 2 / Supplementary Fig. 24), the excited-state oxidation potentials of $[Mn(L^{bi})_3]^+$ and $[Mn(L^{tri})_2]^+$ are ca. -1.9 V vs SCE, leading to roughly 1 eV driving-force for photoinduced electron transfer to MV^{2+}. The reductive dechlorination of CCl_4 implies that very challenging photoreductions are within reach. The MLCT luminescence of $[Mn(L^{tri})_2]^+$ is quenched with a rate constant on the order of $3 \cdot 10^9$ M^{-1} s^{-1} by MV^{2+} (Supplementary Information), indicating that photoinduced electron transfer to this acceptor occurs from the MLCT excited state (green box in Fig. 4d). Furthermore, we expect that the photoreduction of CCl_4 also proceeds from the MLCT (rather than the $^3\pi$-π^*) state for thermodynamic reasons, though we have been unable to perform analogous MLCT luminescence quenching studies due to the irreversibility of the electron transfer in this case.

In toluene solutions containing 40 mM anthracene and 25 μM of $[Mn(L^{bi})_3]^+$ or $[Mn(L^{tri})_2]^+$, photoinduced energy transfer is observable (Fig. 5a / Supplementary Fig. 27). Selective excitation of the Mn(I) complexes results in the well-known triplet absorption spectrum of anthracene, which decays with lifetimes of 52-73 μs (Supplementary Fig. 37). Moreover, delayed anthracene fluorescence is detectable as a consequence of triplet-triplet annihilation (Fig. 5b /

Supplementary Fig. 27)[48]. These findings, together with our control experiments, provide unambiguous evidence for triplet-triplet energy transfer. Based on relative actinometry experiments with $[Ru(bpy)_3]^{2+}$ (Supplementary Information), the quantum efficiency of triplet energy transfer under these conditions is 9.4% for $[Mn(L^{bi})_3]^+$ and 12.1% for $[Mn(L^{tri})_2]^+$. The MLCT emission of the Mn(I) complexes remains virtually unquenched, indicating that the energy transfer to anthracene does not directly involve the MLCT state, but instead occurs from the $^3\pi$-π^* state at 2.3 eV (pink box in Fig. 4d).

Photostability and photocatalysis

In preparation of lab-scale photocatalysis experiments with our complexes, we performed photostability studies under long-term LED irradiation at 405 nm (Supplementary Information). In CH_2Cl_2, $[Mn(L^{bi})_3]^+$ is considerably more photo-robust than $[Mn(L^{tri})_2]^+$, and it seems possible that this is related to differences in metal-ligand bonding strengths between the two complexes. In particular, π-backbonding is significantly stronger in $[Mn(L^{bi})_3]^+$ than in $[Mn(L^{tri})_2]^+$ according to infrared spectroscopy, which shows C≡N stretches of 2120 cm^{-1} for both free ligands, compared to 2064 cm^{-1} for $[Mn(L^{bi})_3]^+$ and 2081 cm^{-1} for $[Mn(L^{tri})_2]^+$ (Supplementary Information). Under 440-nm irradiation of 2 mM $[Mn(L^{bi})_3]^+$ in a deaerated CD_2Cl_2 solution containing 50 mM *trans*-stilbene (with a triplet energy of 2.14 eV), the photoisomerization to *cis*-stilbene (Fig. 4f) was completed to 80% in 5 hours (Supplementary Information), whilst a reference solution containing no Mn(I) complex did not show significant conversion. This represents successful proof-of-concept for lab-scale photocatalysis and paves the way for further applications in synthetic photochemistry[49].

Conclusions

The family of Mn(I) isocyanide complexes introduced herein have their lowest MLCT states at significantly higher energies (ca. 0.8 eV) than a recently explored (isoelectronic) Cr(0) isocyanide complex[20], mostly due to the higher metal oxidation state. The development of chelating isocyanide ligands has led to the long-sought MLCT emission from $3d^6$ metal complexes, which has been far more difficult to obtain than in Cu(I) compounds, where the lack of metal-centered excited states eliminates an important nonradiative decay channel.

The photoactive excited states of our Mn(I) isocyanides are sufficiently long-lived for bimolecular reactions, they readily engage in photoinduced electron and energy transfer reactions, and the proof-of-concept for applications in sensitized triplet-triplet annihilation and photocatalysis is made. The observable electron transfer photoreactivity can occur from the emissive MLCT state, whilst the triplet energy transfer photoreactivity originates from a ligand-centered $^3\pi$-π^* state. Unlike the previously studied Cr(0), Mo(0) and W(0) isocyanides[20,38,40,50] the Mn(I) complexes are air-stable, and regeneration of their initial state after photo-oxidation is possible with common sacrificial reagents. This opens greater perspectives for photoredox catalysis and applications in artificial photosynthesis, for example photochemical water reduction or CO_2 fixation. Further developments of Mn(I) coordination chemistry and photophysics seem desirable for this, but the foundations are now laid. The high abundance, low cost and comparatively low toxicity of many of its compounds make manganese a very attractive element.

The finding that MLCT and ligand-centered $^3\pi$-π^* states of our Mn(I) complexes can both be photoactive, including dual emission at 77 K, is unexpected and contrasts typical behavior of precious metal based compounds, where only the MLCT state is usually emissive and photochemically relevant[51]. This fundamental insight complements recent unexpected discoveries concerning the photophysical behavior of first-row transition metal complexes, for example luminescent LMCT states in Fe(III) complexes[16,17] or dual emission from V(III) complexes[52]. It seems that the photophysics and the photochemistry of coordination chemistry is at the verge of a new era, with important implications for diverse fields and applications, ranging from light-emitting devices and dye-sensitized solar cells to synthetic photochemistry, solar fuels production, and phototherapy.

Data availability

All pertinent experimental procedures, materials and methods and characterization data (NMR spectroscopy, electrospray ionization mass spectrometry, X-ray diffraction, as well as optical spectroscopic and electrochemical data) are provided in this article and its Supplementary Information. Crystallographic data for $[ZnCl_2(L^{bi})\cdot 0.5C_2H_4Cl_2]$ have been deposited at the Cambridge Crystallographic Data Centre under deposition number CCDC 2047767. Copies of data can be obtained free of charge from www.ccdc.cam.ac.uk/structures/. Source data for Figs. 2 – 5 are provided with this paper.

References

1 Costa, R. D. *et al.* Luminescent ionic transition-metal complexes for light-emitting electrochemical cells. *Angew. Chem. Int. Ed.* **51**, 8178-8211 (2012).

2 Hagfeldt, A., Boschloo, G., Sun, L. C., Kloo, L. & Pettersson, H. Dye-sensitized solar cells. *Chem. Rev.* **110**, 6595-6663 (2010).

3 Twilton, J. *et al.* The merger of transition metal and photocatalysis. *Nat. Rev. Chem.* **1**, 0052 (2017).

4 Magnuson, A. *et al.* Biomimetic and microbial approaches to solar fuel generation. *Acc. Chem. Res.* **42**, 1899-1909 (2009).

5 Heinemann, F., Karges, J. & Gasser, G. Critical overview of the use of Ru(II) polypyridyl complexes as photosensitizers in one-photon and two-photon photodynamic therapy. *Acc. Chem. Res.* **50**, 2727-2736 (2017).

6 McCusker, J. K. Electronic structure in the transition metal block and its implications for light harvesting. *Science* **363**, 484-488 (2019).

7 Liu, Y. Z., Persson, P., Sundström, V. & Wärnmark, K. Fe N-heterocyclic carbene complexes as promising photosensitizers. *Acc. Chem. Res.* **49**, 1477-1485 (2016).

8 Zhang, W. K. *et al.* Tracking excited-state charge and spin dynamics in iron coordination complexes. *Nature* **509**, 345-348 (2014).

9 Auböck, G. & Chergui, M. Sub-50-fs photoinduced spin crossover in $Fe(bpy_3)^{2+}$. *Nat. Chem.* **7**, 629-633 (2015).

10 Carey, M. C., Adelman, S. L. & McCusker, J. K. Insights into the excited state dynamics of Fe(II) polypyridyl complexes from variable-temperature ultrafast spectroscopy. *Chem. Sci.* **10**, 134-144 (2019).

11 Zhang, K., Ash, R., Girolami, G. S. & Vura-Weis, J. Tracking the metal-centered triplet in photoinduced spin crossover of $Fe(phen)_3^{2+}$ with tabletop femtosecond M-edge X-ray absorption near-edge structure spectroscopy. *J. Am. Chem. Soc.* **141**, 17180-17188 (2019).

12 Chábera, P. *et al.* Fe^{II} hexa N-heterocyclic carbene complex with a 528 ps metal-to-ligand charge-transfer excited-state lifetime. *J. Phys. Chem. Lett.* **9**, 459-463 (2018).

13 Braun, J. D. *et al.* Iron(II) coordination complexes with panchromatic absorption and nanosecond charge-transfer excited state lifetimes. *Nat. Chem.* **11**, 1144-1150 (2019).

14 Duchanois, T. *et al.* NHC-based iron sensitizers for DSSCs. *Inorganics* **6**, 63, doi: 10.3390/inorganics6020063 (2018).

15 Förster, C. & Heinze, K. Photophysics and photochemistry with earth-abundant metals – fundamentals and concepts. *Chem. Soc. Rev.* **49**, 1057-1070 (2020).

16 Chábera, P. *et al.* A low-spin Fe^{III} complex with 100-ps ligand-to-metal charge transfer photoluminescence. *Nature* **543**, 695-699 (2017).

17 Kjær, K. S. *et al.* Luminescence and reactivity of a charge-transfer excited iron complex with nanosecond lifetime. *Science* **363**, 249-253 (2019).

18 Wood, C. J. *et al.* A comprehensive comparison of dye-sensitized NiO photocathodes for solar energy conversion. *Phys. Chem. Chem. Phys.* **18**, 10727-10738 (2016).

19 Young, E. R. & Oldacre, A. Iron Hits the Mark. *Science* **363**, 225-226 (2019).

20 Büldt, L. A., Guo, X., Vogel, R., Prescimone, A. & Wenger, O. S. A tris(diisocyanide)chromium(0) complex is a luminescent analog of Fe(2,2'-bipyridine)$_3^{2+}$. *J. Am. Chem. Soc.* **139**, 985-992 (2017).

21 Mann, K. R. *et al.* Electronic structures and spectra of hexakisphenylisocyanide complexes of Cr^0, Mo^0, W^0, Mn^I, and Mn^{II}. *Inorg. Chim. Acta* **16**, 97-101 (1976).

22 Plummer, D. T. & Angelici, R. J. Synthesis and characterization of homoleptic complexes of the chelating bidentate isocyano ligand *tert*-BuDiNC. *Inorg. Chem.* **22**, 4063-4070 (1983).

23 Treichel, P. M., Firsich, D. W. & Essenmacher, G. P. Manganese(I) and chromium(0) complexes of phenyl isocyanide. *Inorg. Chem.* **18**, 2405-2409 (1979).

24 Hamze, R. *et al.* Eliminating nonradiative decay in Cu^I emitters: >99% quantum efficiency and microsecond lifetime. *Science* **363**, 601-606 (2019).

25 Hossain, A., Bhattacharyya, A. & Reiser, O. Copper's rapid ascent in visible-light photoredox catalysis. *Science* **364**, 450-461 (2019).

26 Di, D. W. *et al.* High-performance light-emitting diodes based on carbene-metal-amides. *Science* **356**, 159-163 (2017).

27 Gernert, M. *et al.* Cyclic (amino)(aryl)carbenes enter the field of chromophore ligands: expanded π system leads to unusually deep red emitting Cu^I compounds. *J. Am. Chem. Soc.* **142**, 8897-8909 (2020).

28 Liu, W. P. & Ackermann, L. Manganese-catalyzed C–H activation. *ACS Catal.* **6**, 3743-3752 (2016).

29 Elangovan, S. *et al.* Efficient and selective N-alkylation of amines with alcohols catalysed by manganese pincer complexes. *Nat. Commun.* **7**, 8 (2016).

30 Mukherjee, A. *et al.* Manganese-catalyzed environmentally benign dehydrogenative coupling of alcohols and amines to form aldimines and H_2: a catalytic and mechanistic study. *J. Am. Chem. Soc.* **138**, 4298-4301 (2016).

31 Sampson, M. D. *et al.* Manganese catalysts with bulky bipyridine ligands for the electrocatalytic reduction of carbon dioxide: eliminating dimerization and altering catalysis. *J. Am. Chem. Soc.* **136**, 5460-5471 (2014).

32 Bourrez, M., Molton, F., Chardon-Noblat, S. & Deronzier, A. Mn(bipyridyl)$(CO)_3$Br : an abundant metal carbonyl complex as efficient electrocatalyst for CO_2 Reduction. *Angew. Chem. Int. Ed.* **50**, 9903-9906 (2011).

33 Henke, W. C., Otolski, C. J., Moore, W. N. G., Elles, C. G. & Blakemore, J. D. Ultrafast spectroscopy of [Mn$(CO)_3$] complexes: Tuning the kinetics of light-driven CO release and solvent binding. *Inorg. Chem.* **59**, 2178-2187 (2020).

34 Zhang, Y. *et al.* Delayed fluorescence from a zirconium(IV) photosensitizer with ligand-to-metal charge-transfer excited states. *Nat. Chem.* **12**, 345-352 (2020).

35 Pal, A. K., Li, C. F., Hanan, G. S. & Zysman-Colman, E. Blue-emissive cobalt(III) complexes and their use in the photocatalytic trifluoromethylation of polycyclic aromatic hydrocarbons. *Angew. Chem. Int. Ed.* **57**, 8027-8031 (2018).

36 Harris, J. P. *et al.* Near-infrared $^2E_g \rightarrow {}^4A_{2g}$ and visible LMCT luminescence from a molecular bis-(tris(carbene)borate) manganese(IV) complex. *Can. J. Chem.* **95**, 547-552 (2017).

37 Drance, M. J. *et al.* Terminal coordination of diatomic boron monofluoride to iron. *Science* **363**, 1203-1205 (2019).

38 Sattler, W., Henling, L. M., Winkler, J. R. & Gray, H. B. Bespoke photoreductants: tungsten arylisocyanides. *J. Am. Chem. Soc.* **137**, 1198-1205 (2015).

39 Mann, K. R., Gray, H. B. & Hammond, G. S. Excited-state reactivity patterns of hexakisarylisocyano complexes of chromium(0), molybdenum(0), and tungsten(0). *J. Am. Chem. Soc.* **99**, 306-307 (1977).

40 Herr, P., Glaser, F., Büldt, L. A., Larsen, C. B. & Wenger, O. S. Long-lived, strongly emissive, and highly reducing excited states in Mo(0) complexes with chelating isocyanides. *J. Am. Chem. Soc.* **141**, 14394-14402 (2019).

41 Harris, R. K. & Mann, B. E. *NMR and the Periodic Table*. (Academic Press, 1978).

42 Brown, A. M., McCusker, C. E. & McCusker, J. K. Spectroelectrochemical identification of charge-transfer excited states in transition metal-based polypyridyl complexes. *Dalton Trans.* **43**, 17635-17646 (2014).

43 Gawelda, W. *et al.* Ultrafast nonadiabatic dynamics of $Fe^{II}(bpy)_3^{2+}$ in solution. *J. Am. Chem. Soc.* **129**, 8199-8206 (2007).

44 Murtaza, Z. *et al.* Energy-Transfer in the Inverted Region - Calculation of Relative Rate Constants by Emission Spectral Fitting. *J. Phys. Chem.* **98**, 10504-10513 (1994).

45 Baba, A. I., Shaw, J. R., Simon, J. A., Thummel, R. P. & Schmehl, R. H. The photophysical behavior of d^6 complexes having nearly isoenergetic MLCT and ligand localized excited states. *Coord. Chem. Rev.* **171**, 43-59 (1998).

46 Taffarel, E., Chirayil, S., Kim, W. Y., Thummel, R. P. & Schmehl, R. H. Coexistence of Ligand Localized and MLCT Excited States in a 2-(2‘-Pyridyl)benzo[g]quinoline Complex of Ruthenium(II). *Inorg. Chem.* **35**, 2127-2131 (1996).

47 Anne, A., Hapiot, P., Moiroux, J., Neta, P. & Savéant, J. M. Oxidation of 10-methylacridan, a synthetic analog of NADH, and deprotonation of its cation radical - convergent application of laser flash-photolysis and direct and redox catalyzed electrochemistry to the kinetics of deprotonation of the cation radical. *J. Phys. Chem.* **95**, 2370-2377 (1991).

48 Singh-Rachford, T. N. & Castellano, F. N. Photon upconversion based on sensitized triplet-triplet annihilation. *Coord. Chem. Rev.* **254**, 2560-2573 (2010).

49 Strieth-Kalthoff, F., James, M. J., Teders, M., Pitzer, L. & Glorius, F. Energy transfer catalysis mediated by visible light: principles, applications, directions. *Chem. Soc. Rev.* **47**, 7190-7202 (2018).

50 Kvapilova, H. *et al.* Electronic excited states of tungsten(0) arylisocyanides. *Inorg. Chem.* **54**, 8518-8528 (2015).

51 Arias-Rotondo, D. M. & McCusker, J. K. The photophysics of photoredox catalysis: a roadmap for catalyst design. *Chem. Soc. Rev.* **45**, 5803-5820 (2016).

52 Dorn, M. *et al.* A vanadium(III) complex with blue and NIR-II spin-flip luminescence in solution. *J. Am. Chem. Soc.* **142**, 7947-7955 (2020).

Acknowledgements

O. S. W. thanks the Swiss National Science Foundation (grant numbers 200021_178760 and 206021_157687) for financial support. C. K. acknowledges a Novartis University of Basel Excellence Scholarship for Life Sciences.

Author contributions

P. H. carried out synthetic, spectroscopic and electrochemical work and analyzed data, C. K. provided guidance in spectroscopic work, designed photochemical studies, and helped in data analysis, C. B. L. provided guidance in synthetic, spectroscopic and electrochemical work, D. H. performed NMR studies, O. S. W. conceived the project and provided guidance. All authors contributed to the writing and editing of the manuscript and have given approval to its final version.

Competing interests

The authors declare no competing interests.

Entry for the table of contents

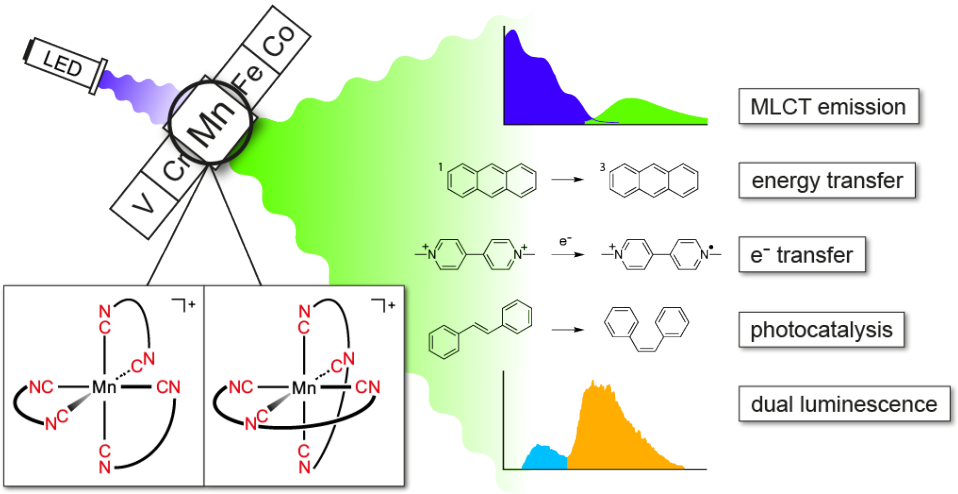

Manganese(I) is isoelectronic to iron(II) but has been typically overlooked as an abundant and cheap metal for the development of $3d^6$ MLCT emitters and photosensitizers. Using a different molecular design than the common polypyridine and carbene ligand framework approaches, air-stable manganese(I) isocyanide complexes exhibiting MLCT luminescence, as well as energy and electron transfer photoreactivity were obtained.